GSC Biological and Pharmaceutical Sciences

eISSN: 2581-3250 CODEN (USA): GBPSC2

Cross Ref DOI: 10.30574/gscbps

Journal homepage: https://gsconlinepress.com/journals/gscbps/

GSC Biological and Pharmaceutical Sciences

GSC Online Press INDIA

(Research Article)

Check for updates

Antibacterial and antioxidant activities of Ag-Mn bimetallic nanoparticles mediated by mango (*Mangifera indica* l.) Leaf extract

Cornelius Tochukwu Nwankwo [1, 2, *], Abdullahi Ishyaku Alhaji [1], Abdulsalami Mohammed Sani [1], Calistus C. Williams [1], Muhammad Alhassan Gabi [2] and Zainab Nasiru Musa [2]

[1] *Department of Biotechnology, Faculty of Science, Nigerian Defence Academy, Kaduna, Nigeria.*

[2] *Department of Biotechnology, Faculty of Computing and Science, Mewar International University, Nigeria.*

GSC Biological and Pharmaceutical Sciences, 2026, 34(03), 179-190

Publication history: Received on 04 February 2026; revised on 20 March 2026; accepted on 23 March 2026

Article DOI: https://doi.org/10.30574/gscbps.2026.34.3.0095

Abstract

This study investigated the synthesis, characterization, antibacterial and antioxidant activities of silver–manganese (Ag–Mn) bimetallic nanoparticles using *Mangifera indica* leaf extract. Ag–Mn nanoparticles were synthesized through a one-pot green synthesis approach and characterized using UV–Vis spectroscopy, FTIR, SEM, and EDX analyses. The antibacterial activities were accessed using the agar well diffusion method and antioxidant activities by DPPH and ABTS assays. The UV–Vis spectra exhibited a distinct surface plasmon resonance peak at 445 nm, confirming the presence of Ag nanoparticles, along with minor peaks attributable to Mn interactions. FTIR analysis revealed functional groups such as hydroxyl, carboxylic, and carbonyl bands that acted as reducing and stabilizing agents. SEM images displayed irregular, non-spherical nanoparticles with moderate aggregation, while EDX confirmed the elemental composition of Ag and Mn. The antibacterial evaluation demonstrated that the Ag–Mn nanoparticles exhibited broad-spectrum activity, with the highest inhibition against *Klebsiella pneumonia* (19.98 ± 1.03mm), followed by *Pseudomonas aeruginosa*, *Salmonella typhi*, and *E. coli*. Antioxidant assays showed that the Ag–Mn NPs showed dose-dependent radical scavenging activity. The ABTS assay outperformed ascorbic acid at concentrations ≤40 μg/mL, with an IC_{50} of 31.25 μg/mL. The DPPH IC_{50} was 23.74 μg/mL, slightly lower than that of ascorbic acid. The synthesized Ag–Mn bimetallic nanoparticles showed strong antibacterial and antioxidant potential, due to the combined impacts of silver and manganese, and the capping influence of phytochemicals in *M. indica* leaf extract. These findings suggest their application in biomedical and pharmaceutical as eco-friendly therapeutic agents.

Keywords: Antibacterial; Antioxidants; Silver-Manganese; Nanoparticles and *Mangifera indica*

1. Introduction

Bimetallic nanoparticles can exhibit enhanced thermal stability, catalytic activity, electronic properties, and antimicrobial effects. These improvements arise from the interaction between the two metals, which often results in unique electronic and structural configurations. Bimetallic nanoparticles can be designed in different architectures, such as core-shell, alloy, or heterostructure, based on the desired application (1). Green synthesis is an eco-friendly method of making nanoparticles using natural materials instead of harmful chemicals. It is called "green" because it's safe for the environment and does not produce toxic byproducts (2). One of the best ways to conduct green synthesis is by using plant extracts, which contain natural chemicals like flavonoids, tannins, alkaloids, and phenols. These chemicals help reduce metal salts, like silver nitrate or manganese chloride, into nanoparticles and also stabilize them so they do not clump together (3). This approach is popular because it is non-toxic, cost-effective, and does not require high temperatures or strong chemicals. It is also scalable for both small and large-scale production (4).

* Corresponding author: Cornelius Tochukwu Nwankwo

Mangifera indica L. commonly known as mango, one of the nutritious tropical fruits, belonging to genus Mangifera and family Anacardiaceae, is employed as the reducing agent for the synthesis of bimetallic NPs. Mango leaves are often positioned alternately on the twigs and range in length from 6 to 16 inches. They have a lathery texture. The juvenile leaves have a pinkish-green hue. Mango leaf extracts have been utilized in traditional medicine and have been shown to have antibacterial, antioxidant, anticancer, and anti-diabetic qualities. Its decoctions have also been used to treat skin burns, colds, asthma, fever, cough, diarrhea, hypertension, and sleeplessness. Additionally, it has been used as an effective herbal mouthwash (5). Including their antipyretic, hypolipidemic, hepatoprotective, anticancer, gastroprotective, and anti-diabetic properties, reported by Badeggi et al. (6).

High amount of phytochemicals, which may offer protection against free radical damage, are largely accumulated in fruits and vegetables (7). *M. indica* has a wealth of bioactive compounds like polyphenols, terpenes, sterols, carotenoids, vitamins and amino acids (8). Mango leaves (*Mangifera indica*) are rich in these natural compounds, making them a great choice for producing silver-manganese (Ag-Mn) bimetallic nanoparticles. Currently, there are only few studies on the green synthesis of bimetallic nanoparticle using *Mangifera indica* L. as capping agent. Thus, this study explored the antibacterial and antioxidant effects of Ag-Mn nanoparticle synthesized by *M. indica* leaf extract.

2. Materials and methods

2.1. Plant Material

Fresh mango (*Mangifera indica*) leaves were collected from the environment of Mewar International University, Nigeria. The leaves were thoroughly washed with distilled water to remove all surface contaminants. After rinsing, the leaves were air-dried at room temperature and subsequently oven-dried at 60°C. The dried leaves were grounded into a fine powder using a mechanical grinder and stored in airtight containers.

2.2. Preparation of Leaf Extract

Crude extraction was prepared following the method described by Ibrahim (9). Specifically, 10 grams of the powdered mango leaf was mixed with 90 milliliters of distilled water. The mixture was heated at 80°C for 60 minutes with continuous stirring. After cooling to room temperature, the extract was filtered using Whatman No. 1 filter paper, which was used as the reducing agent in nanoparticle synthesis.

2.3. Synthesis of Bimetallic Nanoparticles (Ag-Mn NPs)

The synthesis of bimetallic nanoparticles was carried out using the aqueous *M. indica* leaf extract prepared. The method described by Amatya et al. (10) was adopted with slight modifications. 10 mL of freshly prepared *M. indica* leaf extract was added to a mixture containing 10 mL of 1 mM silver nitrate ($AgNO_3$) solution and 10 mL of 0.1 M of Potassium per manganate ($KMNO_4$). The mixture was combined in 1:1 volume ratio (v/v) in a conical flask. The reaction mixture was continuously stirred on a magnetic stirrer at 60 °C for 30 minutes to facilitate reduction and nanoparticles formation. The formation of bimetallic nanoparticles was visually confirmed by a gradual colour change, indicating the successful reduction of metal ions. The synthesized nanoparticles were subsequently collected by centrifugation at 10,000 rpm for 15 minutes. Followed by washing of the pellets with distilled water to remove unreacted precursors and phytochemical residues. Finally, it was oven-dried at 60 °C and stored in airtight containers.

2.4. Characterization of the Synthesized Ag-Mn NPs

UV–Visible Spectroscopy was used to investigate the optical properties and surface plasmon resonance (SPR) of the synthesized nanoparticles. The analysis was carried out using a double-beam UV–Vis spectrophotometer (Spectrumlab 110) at wavelengths between 200–800 nm. The nanoparticles samples were appropriately diluted with distilled water and placed in quartz cuvettes before measurement of the absorbance (11).

Fourier Transform Infrared Spectroscopy (FTIR) was performed using a SHIMADZU FTIR-8400S spectrophotometer to identify the functional groups involved in the reduction of the bimetallic nanoparticles. The FTIR spectra, were recorded in the range of 4000–400 cm^{-1}, and analyzed to detect peaks that corresponds to hydroxyl, carbonyl, and other phytochemical-related functional groups (11).

Scanning Electron Microscopy (SEM) and Energy Dispersive X-Ray (EDX) were employed to confirm the morphology and elemental composition of the synthesized nanoparticles (JEOL JCM-6000PLUS coupled with an EX-54450U1S61 detector, OH-USA) on various regions of the samples at 10 keV (12).

2.5. Antibacterial Activity

The method of Mezher et al. (13) was adopted to assess the antibacterial activity of the synthesized Ag-Mn nanoparticles using the agar well diffusion method. Clinical isolates bacterial suspensions namely; *Escherichia coli*, *Klebsiella pneumoniae*, *Salmonella typhi* and *Pseudomonas aeruginosa* were standardized to 0.5 McFarland turbidity and swabbed uniformly on the surface of nutrient agar plates. A cork borer of 6mm diameter was used to make wells on the agar plates and 100 µL of Ag-Mn nanoparticle was added into separate wells. Gentamicin (10 µg/mL) was used as the positive control, while distilled water as the negative control. The plates were incubated at 37°C for 24 hours, after which the zones of inhibition were measured in millimeters. The tests were conducted in triplicate.

2.6. Minimum Inhibitory Concentration (MIC)

The Minimum Inhibitory Concentration (MIC) was determined using the microbroth dilution method in 96-well microtitre plates. Serial two-fold dilutions of the Ag-Mn nanoparticles was prepared in nutrient broth to obtain final concentrations of 6.25 µg/mL, 12.5 µg/mL, 25 µg/mL, 50 µg/mL, and 100 µg/mL. Each well was inoculated with 100µL of the standardized bacterial suspension. The microplates were incubated at 37 °C for 24 hours, and bacteria growth was assessed visually. The MIC was recorded as the least concentration of Ag-Mn nanoparticles that inhibited visible microbial growth, indicating bacteriostatic activity (12).

2.7. Minimum Bactericidal Concentration (MBC)

To ascertain the Minimum Bactericidal Concentration (MBC), 10µL aliquots from wells showing no visible growth in the MIC assay was plated onto freshly prepared nutrient agar plates. These plates were incubated at 37°C for 24 hours. The MBC defined as the lowest concentration of nanoparticles that resulted in no bacteria colony formation on the agar surface, indicating bactericidal activity. This assessment distinguishes between bacteriostatic and bactericidal effects of the synthesized nanoparticles (14).

2.8. 1, 1- diphenyl-2-picryl hydrazyl (DPPH) Radical Scavenging Assay

The DPPH assay was carried out to evaluate the free radical scavenging activity of the synthesized Ag-Mn nanoparticles at different concentrations: 6.25 µg/mL, 12.5 µg/mL, 25 µg/mL, 50 µg/mL, and 100 µg/mL. 0.1 mM. DPPH solution was freshly prepared in methanol. In each reaction tube, 1 mL of DPPH solution was mixed with 1 mL of the nanoparticle sample at the designated concentration. The mixture was incubated in the dark at room temperature for 30 minutes. After incubation, the absorbance of the mixture was measured at 517 nm using a UV–Vis spectrophotometer. A decrease in absorbance indicated an increase in radical scavenging activity. Ascorbic acid, at equivalent concentrations, was used as a reference antioxidant. The percentage inhibition of DPPH radicals was calculated using the formula:

$$Inhibition\ (\%) = \frac{A_0 - A_1}{A_0} \times 100$$

where A_0 is the absorbance of the control (DPPH solution without sample), and A1 is the absorbance of the test sample (4).

2.9. 2,2′-azino-bis (3-ethylbenzothiazoline-6-sulfonic acid (ABTS) Radical Scavenging Assay

The ABTS radical scavenging activity of the Ag-Mn nanoparticles was assessed using a previously prepared ABTS radical cation solution. The $ABTS^+$ solution was generated by mixing 7 mM ABTS stock with 2.45 mM potassium persulfate and the reaction mixture was allowed to stand in the dark at room temperature for 12–16 hours. Before use, the $ABTS^+$ solution was diluted with methanol to an absorbance of 0.70 ± 0.02 at 734 nm. To test antioxidant activity, 1 mL of diluted $ABTS^+$ solution was mixed with 1 mL of Ag-Mn nanoparticle samples at varying concentrations: 20 µg/mL, 40 µg/mL, 60 µg/mL, 80 µg/mL, and 100 µg/mL. The reaction mixtures were incubated in the dark for 10 minutes, and absorbance was measured at 734 nm. Ascorbic acid was used as a positive control. The percentage inhibition was calculated using the same formula as for DPPH. The results from both assays were used to determine the concentration-dependent antioxidant potential of the Ag-Mn nanoparticles (4).

2.10. Statistical Analysis

The Statistical Package for Social Sciences (SPSS) version 25 software was utilized to identify differences between the groups using one-way analysis of variance (ANOVA), Tukey's test, and unpaired T-tests ($p<0.05$).

3. Results

3.1. UV–Vis Spectroscopy of Synthesized Bimetallic Ag–Mn Nanoparticles

The UV–Vis absorption spectra of the synthesized Ag–Mn nanoparticles using *M. indica* leaf extracts revealed characteristic surface plasmon resonance (SPR) peaks within the visible region. It showed prominent absorption bands between 440–460 nm, which confirms the successful formation of silver-based nanoparticles. The SPR peak is a sigmoid optical property of metallic nanoparticles and indicates the collective oscillation of conduction electrons upon interaction with light.

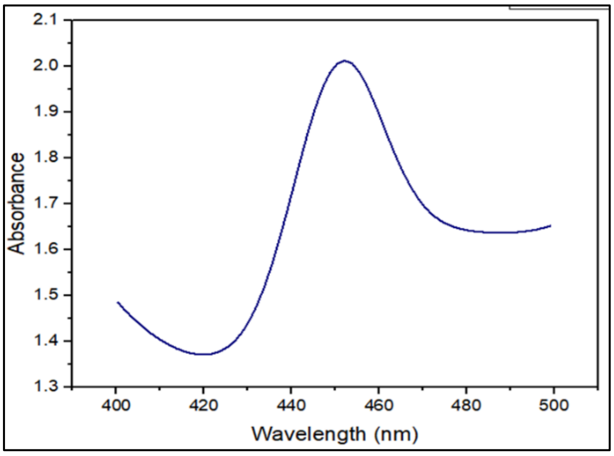

Figure 1 UV–Vis Spectroscopy of Synthesized Bimetallic Ag–Mn Nanoparticles

3.2. FTIR Spectroscopy of Synthesized Bimetallic Ag–Mn Nanoparticles

Table 1 and figure 2 presents the FTIR spectrum of the synthesized Ag–Mn nanoparticles which showed several absorption bands that confirmed the presence of bioactive phytochemicals from *M. indica* leaf extract acting as natural reducing and stabilizing agents. Peaks around 3279.5 cm^{-1} and 1109.9 cm^{-1} revealed the presence of hydroxyl and ether groups, likely from polyphenols and flavonoids. The band at 1650.9 cm^{-1} suggests carbonyl or aromatic C=C stretching, common in plant secondary metabolites. The band at 2504.2 cm^{-1} further supports the presence of carboxylic acids, which may coordinate with Ag^{+} and Mn^{2+} ions. These spectral features indicate that *M. indica* leaf extract enhanced the reduction of metal ions and also provided functional groups for stabilizing the synthesized Ag–Mn nanoparticles.

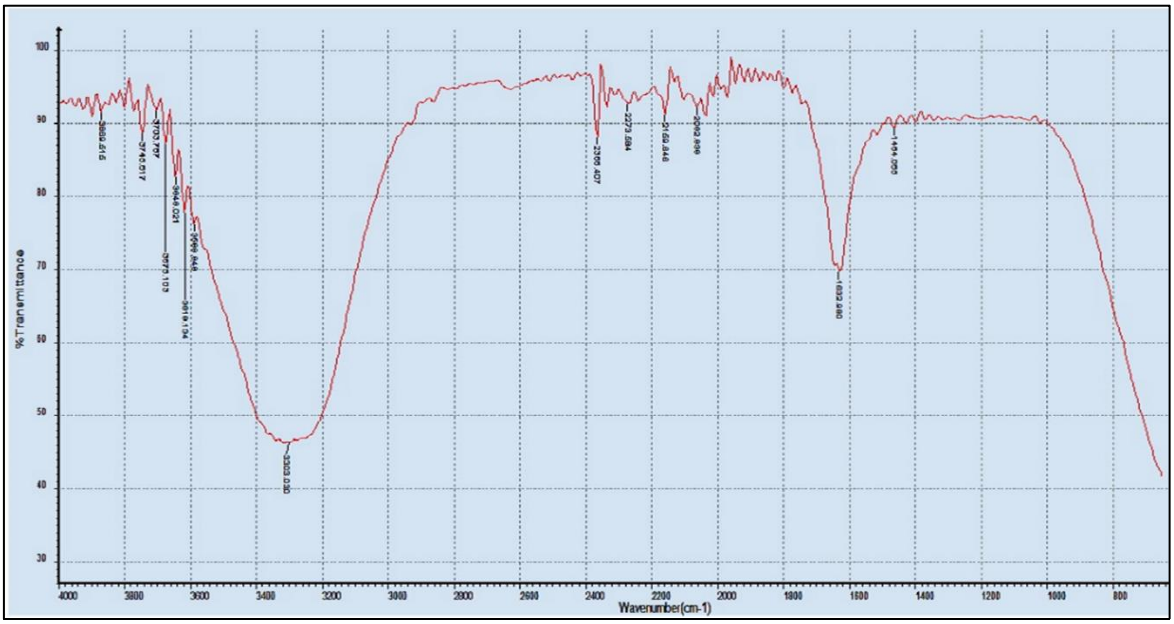

Figure 2 FTIR result of Ag–Mn Nanoparticles Synthesized Using *M. indica* leaf extract

Table 1 FTIR Spectroscopy of Ag–Mn Nanoparticles

Wavenumber (cm^{-1})	Bond Type	Functional Group
3748	O–H stretch (sharp)	Free hydroxyl (alcohols, phenols)
3285	N–H stretch (medium)	1° or 2° amines, amides
2665	O–H stretch (broad)	Carboxylic acids (hydrogen-bonded OH)
2364	C–H overtone or combo	Typically attributed to atmospheric CO_2
2158	C≡C stretch (weak)	Alkynes (internal)
1968	C=O	carbonyl groups (complex carbonyl compounds)
1628	C=C stretch (medium)	Alkenes or aromatic C=C (in conjugated systems)

3.3. SEM –EDX Ag–Mn nanoparticles

Figure 3 presents the SEM micrograph of Ag–Mn nanoparticles synthesized using mango leaf extract at a magnification of ×1500. The image reveals a dense distribution of star-like crystalline nanostructures, indicating uniform synthesis and dispersion across the substrate surface. These structures suggest well-formed nanoparticle agglomerates with distinct morphology, likely influenced by the phytochemical constituents of the *M. indica* leaf extract. The overall particle dispersion is fairly homogeneous, and the absence of large clusters suggests good stabilization by the bioactive compounds during synthesis. The EDX Spectrum displayed a vast array of elemental composition of the synthesized Ag-Mn Nanoparticles. With carbon having highest weight (55.05%) and phosphorus the least (0.06%).

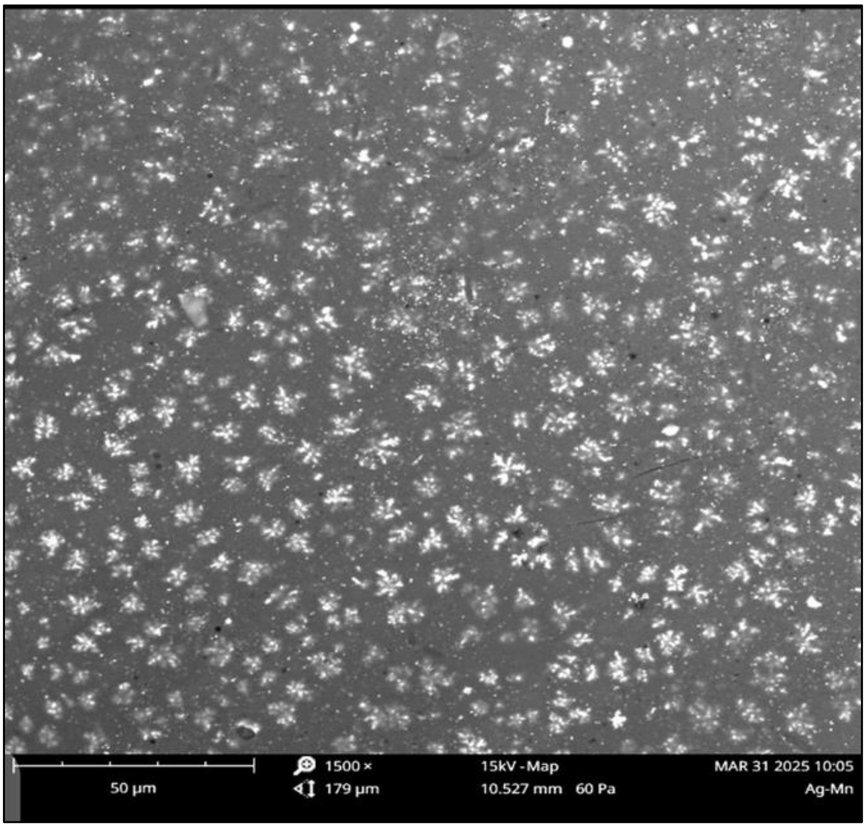

Figure 3 SEM micrograph of Ag–Mn nanoparticles synthesized using mango leaf extract (x1500)

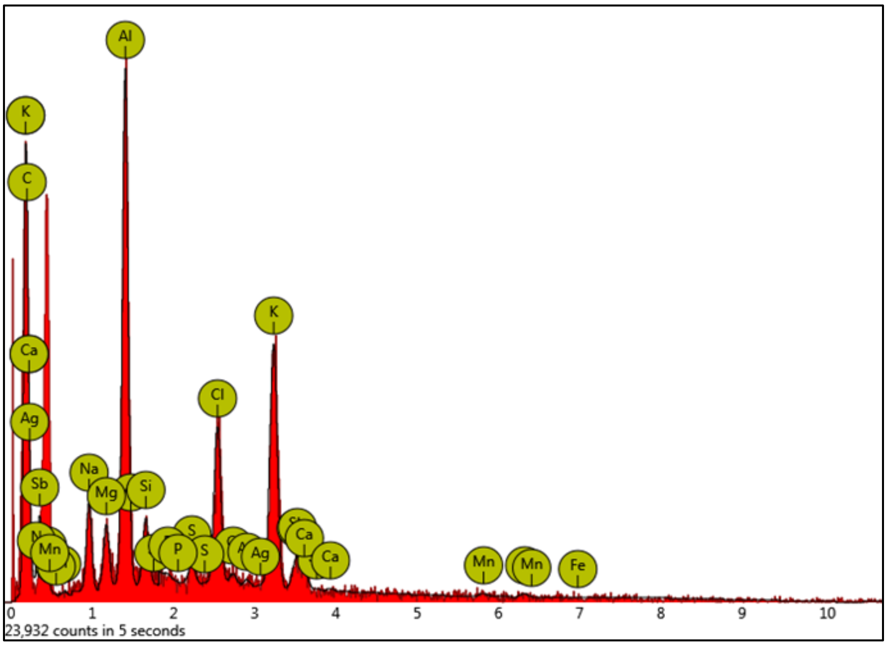

Figure 4 EDX Spectrum of Ag-Mn Nanoparticles

Table 2 Elemental composition of Ag-Mn Nanoparticles

Element Number	Element Symbol	Element Name	Atomic Concentration	Weight Concentration
6	C	Carbon	71.70	55.05
13	Al	Aluminium	6.48	11.17
19	K	Potassium	4.09	10.21
7	N	Nitrogen	11.19	10.02
17	Cl	Chlorine	2.17	4.91
11	Na	Sodium	1.53	2.24
14	Si	Silicon	0.88	1.58
12	Mg	Magnesium	0.87	1.35
20	Ca	Calcium	0.41	1.06
47	Ag	Silver	0.12	0.85
26	Fe	Iron	0.16	0.57
16	S	Sulfur	0.27	0.55
25	Mn	Manganese	0.11	0.38
15	P	Phosphorus	0.03	0.06

3.4. Antibacterial activity of Ag-Mn NPs synthesized

Table 3 presents the zones of inhibition (Mean ± SD) of Ag–Mn nanoparticles synthesized from mango leaf extracts against four bacterial isolates. The results showed that both nanoparticle variants possess moderate antibacterial activity, with varying effectiveness depending on the organism tested. Ag–Mn nanoparticles showed the highest inhibition against *Salmonella typhi* (14.33 ± 1.15 mm) and *Escherichia coli* (12.00 ± 0.40 mm), indicating stronger antibacterial potential with *M. indica* leaf extract alone. In contrast, Ag–Mn nanoparticles were more effective against

Pseudomonas aeruginosa (19.33 ± 0.58 mm) and *Klebsiella pneumoniae* (19.98 ± 1.03 mm). The positive control (PC), gentamicin, exhibited significantly higher zones of inhibition across all bacteria, such as 27.50 ± 0.50 mm for *E. coli* and 29.30 ± 0.30 mm for *Klebsiella pneumoniae*, confirming its superior antimicrobial potency. The negative control (NC), using distilled water, showed no inhibition (0.00 mm), validating that the observed antibacterial effects were due to the nanoparticle formulations.

Table 3 Zones of Inhibition of Ag–Mn Nanoparticles and Controls Against Bacterial Isolates

Samples	*Escherichia Coli*	*Salmonella Typhi*	*Klebsiella pneumoniae*	*Pseudomonas aeruginosa*
Ag-Mn NPs	12.00 ± 0.40^{a}	14.33 ± 1.15^{a}	19.98 ± 1.03^{a}	19.33 ± 0.58^{a}
Positive Control (Gentamicin)	27.50 ± 0.50^{b}	27.17 ± 0.76^{b}	29.30 ± 0.30^{b}	27.33 ± 0.58^{b}
Negative Control (Distilled water)	0.00±0.00	0.00±0.00	0.00±0.00	0.00±0.00

Values are presented as Mean ± SD, n = 3, values down the column with different superscript are significantly different at the $p<0.05$

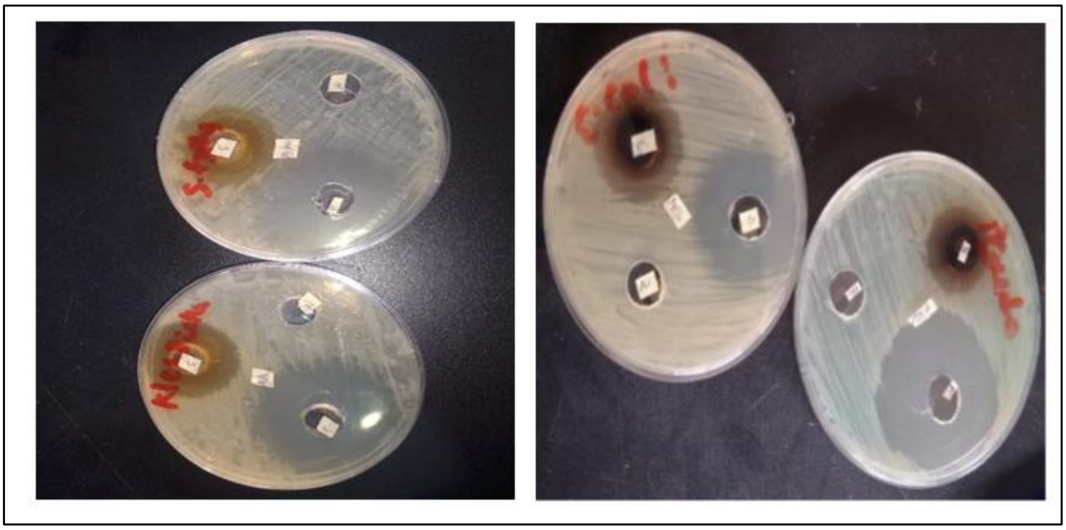

Figure 5 Antibacterial Activities of Ag-Mn Bimetallic Nanoparticle against *E. coli, S. typhi, K. pneumoniae, P. aeruginosa* and standard Gentamicin

3.5. Minimum Inhibitory Concentration (MIC) and Minimum Bactericidal Concentration (MBC)

Ag-Mn nanoparticle exhibited an MIC of 12.5 µg/mL for all tested bacteria, showing equal inhibitory strength irrespective of the synthesis source. The MIC and MBC values remained identical for all bacteria tested.

Table 4 MIC and MBC of Ag-Mn Nanoparticles

Isolates	MIC	MBC
E. coli	12.5 µg/mL	25 µg/mL
S. typhi	12.5 µg/mL	25 µg/mL
Klebsiella pneumonia	12.5 µg/mL	12.5 µg/mL
P. aeruginosa	12.5 µg/mL	25 µg/mL

3.6. DPPH Radical Scavenging Activity of Ag–Mn Nanoparticles

Table 5 presents the antioxidant activity of Ag–Mn nanoparticles synthesized using *M. indica* leaf extract compared with ascorbic acid as the standard. The results showed a concentration-dependent increase in radical scavenging activity across all samples: Ag-Mn NPs exhibited the most consistent performance, increasing from 39.53 ± 0.09% at 6.25 μg/mL to a maximum of 65.12 ± 0.10% at 100 μg/mL, indicating strong antioxidant potential. Ascorbic acid (standard), as expected, demonstrated the highest antioxidant activity, starting at 15.58 ± 0.61% and reaching 78.34 ± 0.06% at 100 μg/mL.

3.7. ABTS Radical Scavenging Activity of Ag–Mn Nanoparticles

The antioxidant activity of Ag–Mn nanoparticles prepared with *M. indica* leaf extract and ascorbic acid as the reference is shown in Table 6. All samples exhibited a concentration-dependent rise in radical scavenging activity: Ag-Mn NPs exhibited the most consistent performance, increasing from 53.49 ± 0.23% at 20μg/mL to a maximum of 59.63 ± 0.25% at 100 μg/mL, indicating strong antioxidant potential. Ascorbic acid (standard), demonstrated slightly lower antioxidant activity than the Ag-Mn, starting at 50.46 ± 0.72% and reaching 55.21 ± 0.25% at 100 μg/mL.

3.8. IC_{50} Values of DPPH and ABTS Activity of Ag–Mn Nanoparticles

The IC_{50} values present the concentration required to scavenge 50% of free radicals. For the DPPH assay, Ag–Mn NPs showed an IC_{50} of 23.74μg/mL, while ascorbic acid had a lower IC_{50} of 34.56μg/mL, this showed higher potency. In contrast, the ABTS assay revealed stronger activity for the nanoparticles, with an IC_{50} of 31.25μg/mL compared to 8.83 μg/mL for ascorbic acid. These results confirm that Ag–Mn NPs possess notable antioxidant potential, especially in the ABTS system, likely due to effective phytochemical capping from mango leaf extract.

Table 5 DPPH Antioxidant Activity (Ag/Mn NPs) and Ascorbic Acid

Concentration (μg/mL)	% Inhibition Ag-Mn NPs	% Inhibition Ascorbic acid
6.25	39.53 ± 0.09^{a}	15.58 ± 0.61^{b}
12.5	52.99 ± 0.06^{a}	39.83 ± 0.67^{b}
25	48.69 ± 1.36^{a}	59.06 ± 0.11^{b}
50	60.34 ± 0.17^{a}	69.26 ± 0.20^{b}
100	65.12 ± 0.10^{a}	78.34 ± 0.06^{b}

Values are presented as Mean ± SD, n = 3. At $p<0.05$, values in the same row with different superscripts differ significantly.

Table 6 ABTS Antioxidant Activity (Ag/Mn NPs) and Ascorbic Acid

Concentration (μg/mL)	% Inhibition Ag-Mn NPs	% Inhibition Ascorbic acid
20	53.49 ± 0.23^{a}	50.46 ± 0.72^{b}
40	58.02 ± 0.10^{a}	51.74 ± 0.96^{b}
60	57.19 ± 1.06^{a}	54.07± 0.87^{b}
80	58.89 ± 0.44^{a}	54.96 ± 0.58^{b}
100	59.63 ± 0.25^{a}	55.21 ± 0.25^{b}

Values are presented as Mean ± SD, n = 3. At $p<0.05$, values in the same row with different superscripts differ significantly.

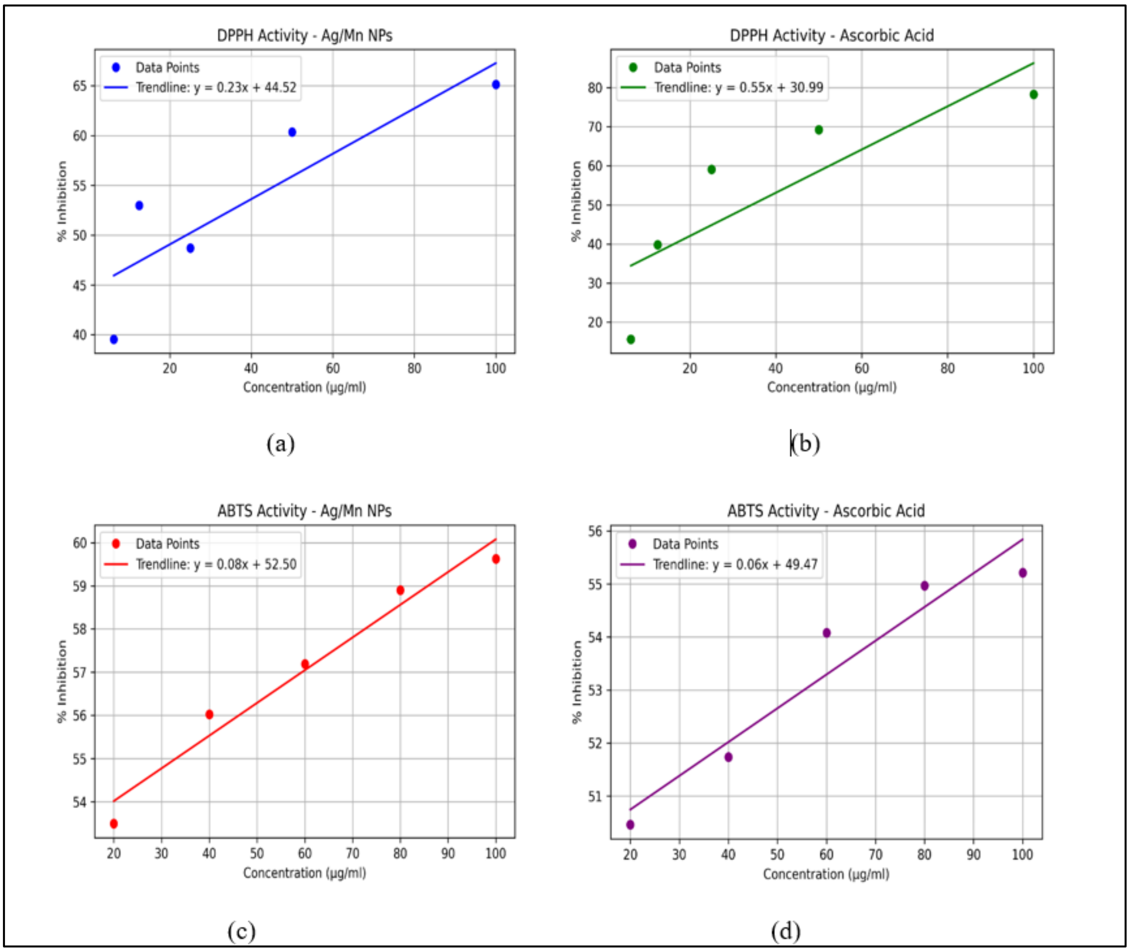

Figure 6 Regression Coefficients of Antioxidants Concentrations of Ag-Mn NPs

Table 7 IC_{50} of DPPH and ABTS Activity of Ag–Mn Nanoparticles

Assay	Samples	Equation	IC_{50} (μg/mL)
DPPH	Ag-Mn	y = 0.23x + 44.52	23.74
DPPH	Ascorbic Acid	y = 0.55x + 30.99	34.56
ABTS	Ag-Mn	y = 0.08x + 52.50	31.25
ABTS	Ascorbic Acid	y = 0.06x + 49.47	8.83

4. Discussion

The UV–Vis spectroscopy analysis of the synthesized silver-manganese (Ag–Mn) bimetallic nanoparticles showed a strong absorption peak at approximately 455nm (Figure 1). This peak corresponds to the surface plasmon resonance (SPR) typically observed in silver nanoparticles, indicating successful formation of metallic nanostructures. The position of the SPR band within the 450–460 nm range suggests that silver is the dominant component, but the slight shift from the conventional 420–440 nm range, seen in monometallic silver nanoparticles may be attributed to the incorporation of manganese, particle size distribution, or possible alloying effects. This collaborates with the observations of Drummer et al. (15), who reported a similar red-shift in SPR when manganese was introduced into silver nanoparticle systems synthesized using *Moringa oleifera* extract. Likewise, Daimari et al. (16) noted comparable spectral features in Ag-based bimetallic nanoparticles and linked them to electronic interactions between the metals and surrounding biomolecules.

The FTIR spectral analysis further supports the successful green synthesis of Ag–Mn nanoparticles by identifying functional groups derived from the mango leaf extract that likely played roles in reduction and stabilization. Notable peaks were observed at 3748 cm^{-1}, 3285 cm^{-1}, and 2665 cm^{-1}, corresponding to O–H and N–H stretching vibrations from alcohols, phenols, and amides. These groups are commonly found in phytochemicals such as flavonoids and polyphenols. The peak at 2158 cm^{-1} is feature of C≡C triple bonds from alkynes, while the bands at 1968 cm^{-1} and 1628 cm^{-1} indicate the presence of carbonyl (C=O) and aromatic C=C groups, respectively. These functional groups are indicative of bioactive compounds in the *M. indica* leaf extract that may have acted as both reducing and capping agents during nanoparticle synthesis. In comparison, Yadav and Vohra (17), reported the vibration of O–H groups of polyphenols in biogenic nanomaterials at 3439 cm^{-1}, 2916 cm^{-1}, and 1636 cm^{-1}, attributing these signals to phenolic and flavonoid compounds responsible for reduction and stabilization processes. Similarly, Taibi et al. (18) reported similar FTIR features in their synthesis of silver nanoparticles using *Ulva lactuca* extract, with prominent peaks at 3412 cm^{-1} (O–H), 2923 cm^{-1} (C–H), 1634 cm^{-1} (C=O), and 1033 cm^{-1} (C–O stretch), indicating the presence of phenolic and carbonyl groups involved in nanoparticle formation.

The scanning electron microscopy (SEM) micrograph of the synthesized silver-manganese (Ag–Mn) bimetallic nanoparticles (Figure 3) at ×1500 magnification reveals a dense distribution of uniformly shaped nanostructures with visible dendritic or star-like morphology. This morphological pattern is often associated with bimetallic nanoparticle systems where varying nucleation rates between the two metal precursors, silver and manganese can lead to complex crystal growth structures. The uniformity in distribution suggests that the mango leaf extract provided a consistent reducing and capping environment, leading to stable and well-dispersed nanoparticles. Similar dendritic and dispersed morphologies have been reported by Mohammed and Hawar (19), who synthesized Ag–Mn nanoparticles using *Moringa oleifera* and observed evenly distributed snow like structures attributed to phytochemical-mediated stabilization.

The accompanying energy-dispersive X-ray spectroscopy (EDS) analysis confirmed the elemental composition of the nanoparticles. A significant presence of carbon (71.70 %) and nitrogen (11.19 %) was observed, which is consistent with the occurrence of organic phytochemicals in the mango leaf extract acting as capping agents. Trace metals such as silver (0.12 %) and manganese (0.11 %) were detected, confirming the formation of Ag–Mn nanoparticles. Other elements were identified, likely originating from intrinsic plant metabolites or residual salts from the precursor solutions. These EDX analysis are in agreement with the results of Aldabaan et al. (20), who synthesized Zinc Oxide Nanoparticles from *Psidium guajava* Stem Extract and recorded carbon and nitrogen as dominant signals in their EDX data, with silver signals confirming successful metal incorporation.

The Ag–Mn bimetallic nanoparticles showed a moderate antibacterial activity, although the performance of Ag–Mn nanoparticles is notable given their green synthesis route and potential reduced toxicity. The effects of the nanoparticles on the bacterial isolates are in line with those of Rolim et al. (21), who used green tea leaf extract to synthesize AgNPs and reported MIC values of 3.9–7.8 μg/mL and inhibition zones around 10–15 mm for Gram-negative pathogens, including *E. coli* and *K. pneumoniae*. Although the MIC of this study is slightly higher (12.5 μg/mL), the inhibition zones against *E. coli* (12 mm) and *K. pneumoniae* (20 mm) fall within or exceed that range. Furthermore, Synergistic antibacterial activity studies by Hao et al. (22) revealed that bimetallic nanoparticles often outperform monometallic analogues, with zones of inhibition for *E. coli* approximately 18 mm.

The Ag–Mn bimetallic nanoparticles have a strong antioxidant activity in both the DPPH and ABTS assays, even exceeding that of ascorbic acid at certain concentrations, also revealed a dose-dependent behaviour in both assays. These results align with previous studies on green-synthesized Ag nanoparticles by Singh et al. (23) AgNP antioxidant assays and reported typical DPPH IC_{50} values in the range of 34–50 μg/mL. Gupta et al. (24) reported similar trend of antioxidant in their study which align well with 23.74 μg/mL obtained in this study.

5. Conclusion

This study demonstrated the green synthesis of silver–manganese (Ag–Mn) bimetallic nanoparticles using mango leaf extracts. The UV–Vis, FTIR, and SEM analyses confirmed the formation, functionalization, and structure of the synthesized nanoparticles. The Ag–Mn nanoparticles revealed moderate antibacterial activity and dose-dependent antioxidant potential. It revealed a lower IC_{50} value, indicating stronger biological activity. These results obtained in this study validates the potential of leaves phytochemicals as eco-friendly agents for nanoparticle synthesis with promising biomedical applications.

Compliance with ethical standards

Disclosure of conflict of interest

The authors declare no conflict of interest

References

[1] Kalakonda, P., Mandal, P., Laxmi Mynepally, S., Bashipangu, A., Kethavath, A., Khanam, S. J., & Podila, B.B. (2024). Comparison of multi-metallic nanoparticles-alternative antibacterial agent: understanding the role of their antibacterial properties. Journal of Inorganic and Organometallic Polymers and Materials, 34(5), 2203-2218.

[2] Sharma, R. K., Yadav, S., Dutta, S., Kale, H. B., Warkad, I. R., Zbořil, R. & Gawande, M. B. (2021). Silver nanomaterials: synthesis and (electro-photo) catalytic applications. Chemical Society Reviews, 50(20), 11293-11380.

[3] Shafey, A.M.E. (2020). Green synthesis of metal and metal oxide nanoparticles from plant leaf extracts and their applications: A review. Green Processing and Synthesis, 9(1), 304-339.

[4] Savan Donga & Sumitra Chanda (2021). Facile green synthesis of silver nanoparticles using *Mangifera indica* seed aqueous extract and its antimicrobial, antioxidant and cytotoxic potential (3-in-1 system), Artificial Cells, Nanomedicine, and Biotechnology, 49:1, 292-302, DOI: 10.1080/21691401.2021.1899193

[5] Muralikrishna, T., Malothu, R., Pattanayak, M. & Nayak, P.L. (2014). Green Synthesis of Gold Nanoparticles using *Mangifera indica* (Mango Leaves) Aqueous Extract. World Journal of Nano Science & Technology, 3(2): 66–73.

[6] Badeggi, U. M., Muhammad, B. L,Shaba, F. A., Muhammad, A. M., Muhammad-Idris, H. L, Sulaiman, S. R., Azeh, Y. & Musah, M. (2024). Production and Characterization of Anti-Diabetic Gold Nanoparticles Using the Leaf Extract of *Mangifera indica*, FUDMA Journal of Sciences (FJS), 8(6);455 - 460 DOI: https://doi.org/10.33003/fjs-2024-0806-2965 ISSN online: 2616-1370

[7] Hussen Endris Muhie & Endalew Sisay Awoke (2023). In vitro antioxidant and free-radical scavenging activities of polar leaf extracts of *Vernonia amygdalina*, BMC Complementary Medicine and Therapies, 23:146, 2-12. https://doi.org/10.1186/s12906-023-03923-y

[8] Ediriweera M.K., Tennekoon K.H. & Samarakoon S.R. (2017). A review on ethnopharmacological applications, pharmacological activities, and bioactive compounds of *Mangifera indica* (Mango). Evid Based Complement Alternat Med.:6949835.

[9] Ibrahim, H. M. M. (2015). Green synthesis and characterization of silver nanoparticles using banana peel extract and their antimicrobial activity against representative microorganisms. Journal of Radiation Research and Applied Sciences, 8(3), 265–275.

[10] Amatya S. P., Shrestha, S. & Aryal Y. (2021). Green Approach for Synthesis of Manganese Nanoparticle using Banana Peel (*Musa paradiasca*) and its Characterization. Amrit Research Journal, 2(01), 75-82.

[11] Darwich N.A., Mezher, M., Abdallah, A.M., El-Sayed, A.F., El Hajj, R., Hamdalla, T.A. & Khalil, M.I. (2024). Biosynthesis; Characterization; and Antibacterial, Antioxidant, and Docking Potentials of Doped Silver Nanoparticles Synthesized from Pine Needle Leaf Extract. Processes, 12, 2590. https://doi.org/10.3390/pr12112590

[12] Temesgen Achamo Orshiso, Enyew Amare Zereffa, Ananda Murthy H. C., Taye B. Demissie Suresh Ghotekar, Khanderao Pagar & Onkar Pardeshi (2024). One-Pot Biopreparation of Trimetallic ZnO–MgO–CuO Nanoparticles: Enhanced Cytotoxicity, Antibacterial Activities and Molecular Docking, Chemistry Africa, 7:1963–1980 https://doi.org/10.1007/s42250-023-00830-0

[13] Mezher, M., Hajj, R.E. & Khalil, M. (2022). Investigating the antimicrobial activity of essential oils against pathogens isolated from sewage sludge of southern Lebanese villages. GERMS, 12, 488–506.

[14] Escárcega-González Carlos Enrique, JA Garza-Cervantes, A Vázquez-Rodríguez, Liliana Zulem Montelongo-Peralta, MT Treviño-González, E Díaz Barriga Castro, EM Saucedo Salazar, RM Chávez Morales, DI Regalado Soto, FM Treviño González, JL Carrazco Rosales, Rocío Villalobos Cruz & José Rubén Morones-Ramírez (2018). In vivo antimicrobial activity of silver nanoparticles produced via a green chemistry synthesis using *Acacia rigidula* as a reducing and capping agent, International Journal of Nanomedicine, 13 2349–2363. https://www.dovepress.com

[15] Drummer, S., Madzimbamuto, T., & Chowdhury, M. (2021). Green Synthesis of Transition-Metal Nanoparticles and Their Oxides: A Review. Materials 2021, 14, 2700.

[16] Daimari, J., Basumatary, S., & Deka, A. K. (2024). Bimetallic nanoparticles from coinage metals (Cu, Ag, Au) and its biomedical applications: A Review. Nano-Structures & Nano-Objects, 39, 101247.

[17] Yadav, S., & Vohra, N. (2024). A Comprehensive Review of Silver Nanoparticles: Classification, Synthesis, Properties, Applications, and Toxicity. *Pexacy. com*.

[18] Taibi, M., Aouji, M., Imtara, H., Abujaber, F., Oubihi, A., Ouannou, A. & Hassani, O. (2024). Novel biosynthesis of silver nanoparticles using *Ulva lactuca* and their potential toward environment and agricultural purposes. Frontiers in Sustainable Food Systems, 8, 1490880.

[19] Mohammed, G. M., & Hawar, S. N. (2022). Green biosynthesis of silver nanoparticles from *Moringa oleifera* leaves and its antimicrobial and cytotoxicity activities. International Journal of Biomaterials, 2022(1), 4136641.

[20] Aldabaan, N. A., Morabad, S., Muddapur, U. M., Shaikh, I. A., Dawoud, A., Khan, A. A. & Hussain, S. A. (2024). Antimicrobial Assessment of Zinc Oxide Nanoparticles Synthesized from *Psidium guajava* Stem Extract. Science of Advanced Materials, 16(4), 555-562.

[21] Rolim, W. R., Pelegrino, M. T., de Araújo Lima, B., Ferraz, L. S., Costa, F. N., Bernardes, J. S., ... & Seabra, A. B. (2019). Green tea extract mediated biogenic synthesis of silver nanoparticles: Characterization, cytotoxicity evaluation and antibacterial activity. Applied Surface Science, 463, 66-74.

[22] Hao, Z., Wang, M., Cheng, L., Si, M., Feng, Z. & Feng, Z. (2024). Synergistic antibacterial mechanism of silver-copper bimetallic nanoparticles. Frontiers in Bioengineering and Biotechnology, 11,1337543.

[23] Singh, R., Hano, C., Tavanti, F. & Sharma, B. (2021). Biogenic Synthesis, Characterization, Antioxidant and Antimicrobial of Silver Nanoparticles Using Flower Extract of *Couroupita guianensis* Aubl. Materials 2021, 14, 6854.

[24] Gupta, P., Rai, N., Verma, A., Saikia, D., Singh, S.P., Kumar, R., Singh, S.K., Kumar, D. & Gautam, V. (2022). Green-Based Approach to Synthesize Silver Nanoparticles Using the Fungal Endophyte *Penicillium oxalicum* and Their Antimicrobial, Antioxidant, and In Vitro Anticancer Potential. ACS Omega 2022, 7, 46653–46673.